

# IMPROVING THE EFFICIENCY OF THERMOELECTRIC GENERATORS BY USING SOLAR HEAT CONCENTRATORS

M. T. de Leon, P. Taatizadeh, and M. Kraft

*University of Southampton; School of Electronics and Computer Science, United Kingdom*

**Abstract** — In this paper, we propose a method of improving the efficiency of thermoelectric generators (TEGs) by using a lens to concentrate heat on the heat source of a TEG. Initial experiments performed using discrete components show about 60mV increase in the amount of voltage generated when using a magnifying lens. Simulation results on the proposed TEG configuration exhibit up to 16% efficiency when the input heat flux is increased to 500 times that of the sun's heat flux. The effects of varying the thermoelement length, width, and membrane diameter on the TEG's performance are also characterized. Lastly, plans to fabricate the device on a SOI wafer in the future are presented.

**Keywords** : Thermoelectric generator, Solar heat concentrator, Carnot efficiency

## I - Introduction

The global energy crisis has paved the way for researchers to explore alternative means of generating power. One approach to providing electrical energy is by direct conversion of heat to electrical power with the use of thermoelectric generators (TEGs). It is attractive to use TEGs because they have no mechanical parts; hence resulting in an alternative power system that is silent, stable, reliable, environment-friendly, and possess virtually unlimited lifetime [1, 2].

The basic principle behind the operation of a TEG is the Seebeck effect. The Seebeck effect produces voltage when a temperature difference is applied between the junctions of two different materials. For a TEG to supply a significant amount of power, several thermocouples are connected electrically in series and thermally in parallel. Unfortunately, TEGs typically have low Carnot efficiency described by the equation below,

$$\eta_c = (T_h - T_c)/T_h \quad (1)$$

where  $T_h$  and  $T_c$  are the temperatures at the hot and cold sides, respectively. A typical Peltier device exhibits only about 5-8% efficiency.

By utilizing a solar heat concentrator in conjunction with a TEG, the temperature difference across the thermoelements can be increased; subsequently improving the TEG's efficiency. Figure 1 illustrates this innovation with the lens concentrating solar heat at the center of the TEG's membrane. A similar concept of focusing light onto a lens to provide the required actuation energy in powering up a micro-actuator using photo-thermal-mechanical energy transformation was proposed in [3] but their design was not fabricated.

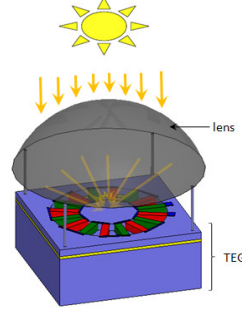


Figure 1: Illustration of proposed TEG with solar heat concentrator system.

Suppose the sun uniformly irradiates an energy density  $q_s$  onto the lens and that the lens has a convex surface area  $A_L$ , then the heat power density  $q_h$  of the incoming heat flux to the TEG's membrane is given by:

$$q_h = \frac{A_L}{A_h} q_s \quad (2)$$

where  $A_h$  is the area of the heated surface at the TEG's membrane. With this approach, we can generate an input heat flux in the order of hundreds of  $\text{kW/m}^2$ . Based on the general heat transfer equation [4], an increase in the input heat flux would translate to a corresponding increase in the temperature difference across the thermoelements; also resulting in an effective increase in its output voltage given by:

$$V_o = N(\alpha_p - \alpha_n)\Delta T \quad (3)$$

where  $N$  is the number of thermocouples and  $\alpha_p$  and  $\alpha_n$  are the Seebeck coefficients of the p- and n-type thermoelements, respectively.

The main objective of this work then is to present the feasibility of the proposed system by first conducting experiments using commercially-available lenses and a TEG module. Heat transfer simulations of the proposed system are also performed to validate the improvement in the efficiency of the TEG. Plans to fabricate an integrated lens and TEG system for future work are also presented. This microscale system has promising applications in on-board power sources, sensor networks, and autonomous microsystems.

## II – Preliminary Experiment and Results

As proof of concept, we first verified the functionality of using a magnifying lens as the solar heat concentrator of a commercially-available TEG unit. To perform the experiment, a Farnell MCPE1-12707AC-S Peltier TEG unit is placed over the center of a Farnell 395-1AB heat sink. A 5x magnifying lens is then

positioned over the TEG keeping a distance equivalent to its focal length to give the best solar heat concentration ratio. To monitor the temperature changes, one thermocouple wire is glued to the middle of the TEG unit and another wire is glued 1cm away. The output terminals of the TEG are connected to a digital multimeter that displays the value of the generated voltage.

Figure 2 shows a plot of the system's output voltage with and without the use of a magnifying lens. Two magnifying lenses having diameters of 6cm and 10cm are used. As expected, higher voltage is generated when a lens is used which can only be attributed to a greater temperature difference across the thermocouple junctions of the TEG. Moreover, using the lens with a larger surface area resulted in a higher output voltage. Unfortunately, the thermocouple wires placed on the surface of the TEG unit only gives us an idea of how heat is distributed across the device but not the actual temperature difference across the thermocouple junctions. Nevertheless, the increase in the amount of voltage generated is sufficient to show that the efficiency can be increased by using a heat concentrator.

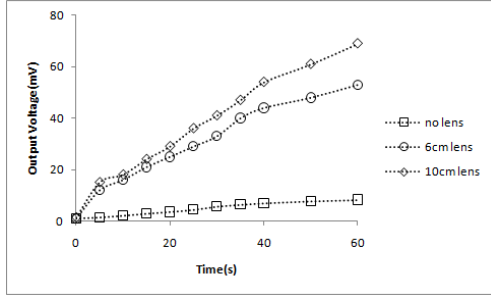


Figure 2: Open circuit output voltage measured with the experiment set-up with and without a magnifying lens.

### III – TEG Design and Simulations

After verifying that the proposed system can be an effective way of improving the efficiency of thermoelectric generators using discrete components, its application at the micro level is investigated. Micro-thermoelectric generators are classified based on the direction of heat flow through the device and on the layout orientation of the thermocouples during fabrication [5]. We chose to focus on the lateral/lateral type of TEGs because it is the simplest to fabricate and has the most potential for CMOS integration.

The configuration of the proposed TEG, shown in figure 3, is similar to the one proposed in [6] where the SOI wafer's device layer is utilized for the suspended membrane and thermoelements. The membrane acts as the heat source of the TEG while the substrate acts as the heat sink. The suspended membrane is circular in geometry to insure optimum transfer of heat from the center of the membrane to the tip of the thermoelements. The oxide and substrate layers below the membrane and the thermoelements are to be etched away to provide better thermal isolation and to optimize the heat

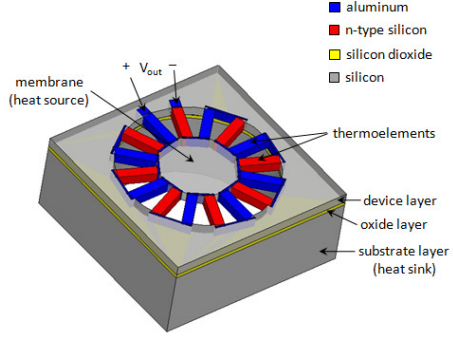


Figure 3: Conceptual design of the TEG device.

flux path so as to obtain the largest temperature difference across the device.

The thermocouple materials are heavily-doped n-type silicon and aluminum. Heavily-doped silicon is seen to be a viable choice for thermoelement material since it has high Seebeck coefficients at doping levels between  $3.5 \times 10^{19} \text{cm}^{-3}$  to  $1.6 \times 10^{20} \text{cm}^{-3}$  [7, 8]. A high doping level is also preferred because the electrical resistivity of silicon decreases with increasing dopant concentration; thus providing a smaller series resistance to the TEG device. It is preferred that both thermoelements use doped silicon but to minimize the number of masks needed during fabrication, aluminum is selected for the second thermoelement instead. The electrical and thermal properties of the two thermocouple materials are listed in table 1. The assumed dopant concentration of the n-type silicon thermoelement is  $5 \times 10^{19} \text{cm}^{-3}$ .

Table 1: Electrical and thermal properties of n-type silicon and aluminum.

Property	n-type silicon	aluminum	references
Seebeck coefficient ( $\mu\text{V/K}$ )	-400	-1.8	[7,9]
Electrical resistivity ( $\Omega\text{-cm}$ )	$2 \times 10^{-3}$	$2.65 \times 10^{-6}$	[6,10]
Thermal conductivity ( $\text{W/mK}$ )	122	237	[6,11]

Heat transfer simulations of the proposed TEG device are performed using COMSOL. The SOI wafer used in the simulations has the following thicknesses:  $500\mu\text{m}$  for the substrate layer,  $5\mu\text{m}$  for the oxide layer, and  $50\mu\text{m}$  for the device layer. Although a thinner device layer is preferred to obtain a larger temperature drop across the thermocouple, a  $50\mu\text{m}$  device layer is selected to ensure mechanical stability of the TEG. Each thermoelectric leg is set to have a length of  $500\mu\text{m}$  and a width of  $20\mu\text{m}$ . Heat transfer by convection is modeled by setting the top and bottom surfaces of the membrane, top surface of the rim, and bottom surface of the substrate to have heat transfer coefficients corresponding to natural external convection with air. The ambient temperature is set to  $20^\circ\text{C}$ . The membrane to be heated located in the middle of the device has a diame-

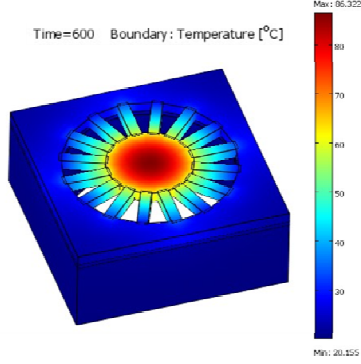


Figure 4: Temperature distribution after 10min for a 1mm x 1mm device with 8 thermocouples. Input heat flux is  $20\text{kW/m}^2$ .

ter of 5mm. The above-mentioned dimensions allow 300 thermocouples to be placed uniformly along the circumference of the membrane with at least  $6\mu\text{m}$  distance between thermoelements. The temperature distribution of a smaller TEG device (1mm x 1mm) is shown in figure 4 to illustrate the heat transfer simulations performed.

For the 10mm x 10mm device simulations, only 16 thermocouples are distributed uniformly along the circumference of the membrane so as to minimize simulation time. We expect that having more thermocouples would decrease the temperature difference across each thermocouple as there is an increase in the area of the heat flux path from the membrane to the rim of the device layer. However, trends in efficiency improvement indicated by changes in  $\Delta T$  should still hold.

To demonstrate the effect of using a heat concentrator, a constant heat flux occupying  $1\text{mm}^2$  is applied at the center of the membrane. The value of the input heat flux is varied from  $50\text{kW/m}^2$  to  $500\text{kW/m}^2$ . With the solar heat flux equivalent to  $1\text{ kW/m}^2$  [12] and based on equation 2, the surface area of the lens is effectively varied from  $50\text{mm}^2$  to  $500\text{mm}^2$ . The results obtained, listed in table 2, clearly shows that the efficiency of the TEG improves with increasing input heat flux. This means that by using a convex lens, the temperature difference across a thermocouple can be increased; resulting in an increase on the TEG's efficiency.

Table 2: Temperature difference and efficiency of 10mm x 10mm TEG with 16 thermocouples for varying input heat flux  $Q$ . Lens surface area is equivalent to  $Q/1000\text{ mm}^2$ .

$Q$ ( $\text{kW/m}^2$ )	$T_c$ (K)	$T_h$ (K)	$\Delta T$ (K)	$\eta_c$ (%)
50	321.482	330.838	9.356	2.828
100	342.356	360.926	18.570	5.145
150	361.222	388.947	27.725	7.128
200	378.943	415.789	36.846	8.862
250	395.894	441.835	45.941	10.398
300	412.279	467.297	55.018	11.774
350	428.227	492.308	64.081	13.016
400	443.823	516.957	73.134	14.147
450	459.132	541.309	82.177	15.181
500	474.199	565.413	91.214	16.132

Simulations are also performed with variations on the dimensions of the thermocouple and on the diameter of the membrane. Higher efficiencies can be achieved by using TEGs with longer lengths and narrower widths. However, the mechanical stability of the TEG after etching out the oxide and substrate layers must also be considered. It is targeted to fabricate different geometries of the device to explore this tradeoff. Characterizations of these variations are exhibited in figures 5-7.

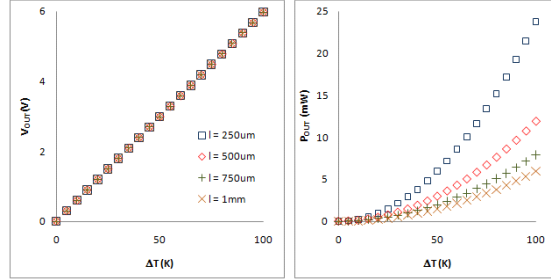


Figure 5: Open circuit output voltage and output power to a matched load for different thermoelement (TE) lengths. TE width is  $20\mu\text{m}$  and membrane diameter is 5mm.

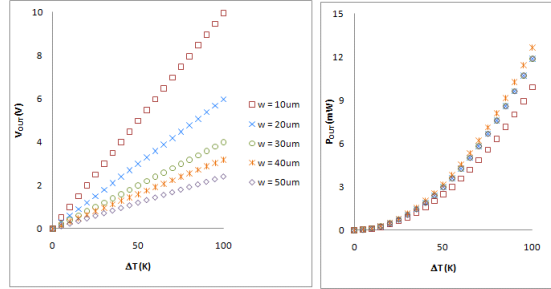


Figure 6: Open circuit output voltage and output power to a matched load for different thermoelement (TE) widths. TE length is  $500\mu\text{m}$  and membrane diameter is 5mm.

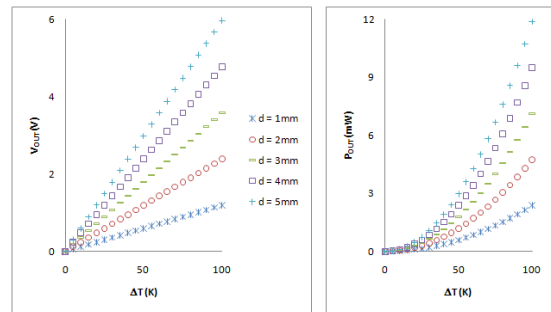


Figure 7: Open circuit output voltage and output power to a matched load for different membrane diameters. Thermoelement length is  $500\mu\text{m}$  and width is  $20\mu\text{m}$ .

Figure 5 shows that the open circuit output voltage versus temperature plot does not change with thermoelement length. It should be noted, though, that the change in temperature increases with the thermoelement length so a longer thermocouple would have a larger temperature difference across it, resulting in a higher output voltage. Meanwhile, a longer thermocouple

results in a higher series resistance, which translates to a lower output power under matched load conditions.

Variations in the thermoelement width shown in figure 6 also imply variations in the number of thermocouples. A wider thermoelement would have lesser number of thermocouples around the 5mm-diameter membrane. Hence, wider thermoelements result in a drop in the output voltage. The supposed reduction in output power due to the drop in the output voltage is offset by the lower series resistance of wider thermoelements, showing minimal variations of the output power to a matched load at different thermoelement widths especially at  $\Delta T$  less than 50K.

Similarly, changing the membrane diameter also means a change in the number of thermocouples of the device. A smaller membrane diameter implies lesser number of thermocouples. Figure 7 shows that a larger membrane diameter results in a higher output voltage and output power. The only limiting factor for the membrane diameter is the structural stability of the device, which is better for smaller membrane diameters.

#### IV – Fabrication

Several 10mm x 10mm TEGs are to be fabricated at the Southampton Nanofabrication Center. The device layer of the SOI wafer should have resistivity in the order of a few  $k\Omega\text{-cm}$  to avoid parasitic resistive coupling between adjacent thermocouples. The fabrication begins by RCA cleaning of the SOI wafer. The next step is doping of the n-type thermoelements by diffusion. Then, the silicon areas of the device layer to be occupied by aluminum as the second thermoelement and for electrical contacts are to be patterned using a negative photoresist and removed by deep reactive ion etching (DRIE). Next, deposition through e-beam evaporation and liftoff of aluminum follow to form the aluminum thermoelements and the electrical connections of the thermocouples. After which, patterning and removal of silicon between thermoelements must be performed by DRIE, forming the gaps between thermoelements. In this step, holes on the membrane are also etched out in preparation of oxide etching. The last step of the TEG fabrication process involves back etching of the substrate and oxide etching by HF vapor phase to release the membrane and the thermoelements.

For the solar heat concentrator, a potential technique for the fabrication of spherical convex lens molds using isotropic wet etching of silicon is presented in [13]. These molds can be subsequently used to fabricate the lenses using hot embossing or UV-molding processes. The lenses to be fabricated are estimated to have a diameter of about 10-15mm to maximize the lens area to heated surface area ratio.

It is also envisioned that an array of these TEGs may be connected in series to boost the open circuit output voltage. Inter-TEG connections in this case may be done internally by including inter-TEG routing in the mask design for aluminum or externally using bond wires. With a TEG array, accurate design of an array of

lenses is also critical for proper heat concentration on each TEG's membrane.

#### V - Conclusions

This work proposes a method of improving the efficiency of thermoelectric generators with the use of solar heat concentrators. Experiments consisting of commercially-available magnifying lenses and a thermoelectric module proved that the use of a heat concentrator generates higher output voltage. Simulation results of a 10mmx10mm TEG device with increasing input heat flux demonstrate an increase in the device's Carnot efficiency. Characterization plots of the output voltage and output power for different thermoelement lengths, widths, and membrane diameters are also discussed as a guide in determining the geometry of several TEGs for fabrication. Fabrication processes under investigation for both TEG and convex lens are also presented.

#### VI - Acknowledgements

M. T. de Leon is supported by the University of the Philippines and the Department of Science and Technology, Philippines.

#### References

- [1] Y. Deng and J. Liu, *Journal of Renewable and Sustainable Energy* 1, 052701, 2009.
- [2] M. Strasser, R. Aigner, C. Lauterbach, T.F. Sturm, M. Franosch and G. Wachutka, *Sensors and Actuators A* 114, pp. 362-370, 2004.
- [3] S. Baglio, S. Castorina, L. Fortuna, and N. Savalli, *Sensors and Actuators A* 101, pp. 185-193, 2002.
- [4] A. Bejan and A. Kraus (editors), *Heat Transfer Handbook*, John Wiley & Sons, 2003.
- [5] W. Glatz, E. Schwyter, L. Durrer, and C. Hierold, *Journal of Microelectromechanical Systems*, vol. 18 no.3, pp. 763-772, 2009.
- [6] R. Egbert, M. Harvey, and B. Otis, *5<sup>th</sup> European Conference on Thermoelectrics*, Ukraine, pp.219-221, 2007.
- [7] F. Salleh, K. Asai, A. Ishida, and H. Ikeda, *Applied Physics Express* 2, 071203, 2009.
- [8] H. Ikeda and F. Salleh, *Applied Physics Letters* 96, 012106, 2010.
- [9] S. Kasap, *Thermoelectric Effects in Metals: Thermocouples*, Web-Materials, pp. 3, 2001.
- [10] *The Physics Hypertextbook*, <http://physics.info>, Accessed last May 2010.
- [11] J. Shackelford and W. Alexander, *CRC Materials Science and Engineering Handbook*, CRC Press, pp. 270-274, 2001.
- [12] R. Amatya and R. Ram, *J. of Electronic Materials* (DOI:10.1007/s11664-010-1190-8), 2010.
- [13] J. Albero, L. Nieradko, C. Gorecki, H. Ottevaere, V. Gomez, H. Thienpont, J. Pietarinen, B. Paivanranta, and N. Passilly, *Optics Express*, vol. 17 no. 8, pp. 6283-6292, 2009.